International Symposium
On Turbulence and Shear Flow
Phenomena (TSFP-9)
June 30 - July 3, 2015 *Melbourne, Australia*

LAGRANGIAN ANALYSIS OF AN IGNITING N-HEPTANE JET AT DIESEL ENGINE RELEVANT CONDITIONS

Alex Krisman
School of Mechanical and Manufacturing Engineering
The University of New South Wales
Kensington, NSW 2052, Australia
a.krisman@unsw.edu.au

Evatt R. Hawkes
School of Mechanical and Manufacturing Engineering
School of Photovoltaics and Renewable Energy Engineering
The University of New South Wales
Kensington, NSW 2052, Australia
evatt.hawkes@unsw.edu.au

Ankit Bhagatwala
Combustion Research Facility
Sandia National Laboratories
Livermore, CA 96551-0969, USA
abhagat@sandia.gov

Mohsen Talei
Department of Mechanical Engineering
University of Melbourne
Parkville, VIC 3010, Australia
mohsen.talei@unimelb.edu.au

Jacqueline H. Chen
Combustion Research Facility
Sandia National Laboratories
Livermore, CA 96551-0969, USA
jhchen@sandia.gov

ABSTRACT

Ignition in diesel engines is incompletely understood due to the extreme thermochemical environment, vigorous turbulence, and their coupling, which are difficult to analyse both experimentally and numerically. In this study, a direct numerical (DNS) was conducted to investigate the ignition process of a relaxed configuration that retains key aspects of diesel ignition. A simplified configuration of a temporally evolving jet of n-heptane at a pressure of 40 atmospheres and an oxidiser temperature of 1100K was selected. The chemistry was represented by a four-step global scheme which is validated against ignition delay time data and reproduces the two-stage autoignition behaviour of n-heptane fuel. The assumptions made are appropriate to reproduce some important features of the gas-phase thermochemistry observed in diesel engines, but lead to a computationally tractable simulation cost. The results show that ignition occurs via both autoignition and deflagration modes of combustion. A two-stage autoignition process leads to the formation of multiple kernels which expand and establish edge-flame deflagrations centered on the stoichiometric mixture fraction surface. The edge-flames propagate throughout the domain and this tends towards a fully-burning solution. Lagrangian passive tracer particles, embedded in the flow, allowed for the identification of the autoignition kernels and the extraction of their statistics and histories. The results show that local mixing histories are highly correlated with the onset of autoignition. In particular, earlier peaks in mixing result in earlier first and second stage autoignition for the igniting kernels.

INTRODUCTION

Diesel engines are widely used in the stationary and transportation energy sectors for their durability, dispatchability and potentially efficient performance. Increasingly stringent standards on pollution formation and the potential regulation of carbon markets have created a demand for improvements to conventional diesel engine design. Historically, the performance of diesel engines has improved substantially via experimental insight and improved conceptual models. However, the information available from experimental studies are limited and further reductions to pollution formation and improvements to fuel conversion efficiency will require a more detailed understanding of the in-cylinder combustion process. Without detailed temporally and spatially resolved data, it is difficult to develop and validate predictive computer models for the engine design process.

Diesel engines operate at very high pressures and temperatures compared to spark-ignition engines and are subject to intense shear-driven turbulence which leads to an extremely large range of length and time scales that need to be resolved. For this reason, direct numerical simulations (DNS) of an actual diesel combustion process are not a tractable option due to the prohibitive computational cost.

Diesel combustion is a topic of increasing research interest. The engine combustion network (ECN), developed by Pickett (2015) is an organisation that exists to coordinate the development of combustion modelling for diesel-like configurations. Standardised experimental databases, typically of reacting spray-flames, are made available and participants can compare the performance of computer mod-

els, as judged by global observables such as ignition delay time and the stabilised lifted flame height, *e.g.*, Pei *et al.* (2013). This effort has assisted the improvement of combustion models in the diesel combustion regime. However, the usefulness of the ECN database is limited by the availability and fidelity of the experimental measurements.

DNS of relaxed configurations can augment the sparse experimental data. By considering simplified configurations, detailed information pertaining to the scalar and velocity fields can be generated in order to gain physical insight and to aid model development.

Here, we consider the case of a gas-phase, temporally evolving jet of normal heptane fuel, represented with four-step global chemistry, igniting at a moderate level of shear-driven turbulence at a diesel-relevant ambient temperature and pressure. This case is designed to represent a diesel relevant autoignitive environment and to investigate the impact of turbulence on the overall ignition process. We do not attempt to capture the spatial development of the jet, multi-phase phenomena, or the correct level of turbulence.

Previous work on laminar lifted by Krisman *et al.* (2015) and igniting mixing layers by Krisman *et al.* (2014) configurations at similar thermochemical conditions revealed some novel features. The laminar lifted flame results showed that stabilised hybrid autoignitive / edge-flame structures could exist, even at nominally autoignitive conditions. These flames exhibited low- and high- temperature autoignition in addition to an edge-flame nature. It was found that adjusting the oxidiser temperature could transition the flame between a purely deflagration to a purely autoignitive feature. The study of ignition in a two-dimensional mixing layer subject to isotropic turbulence revealed a two-stage ignition process that led to the formation of hybrid edge-flame / autoignitive structures. In that case both a two-stage autoignition process and edge-flame deflagration were involved in the overall ignition. However, it was not clear from the two-dimensional studies what role that realistic turbulence would have on the ignition process. A major difference between the previous two-dimensional simulations and the current DNS is the chemical mechanism. Previously, a detailed chemistry for dimethyl ether, as first published by Bhagatwala *et al.* (2015), was used in order to represent the primary features of gas-phase diesel chemistry such as two-stage ignition and the negative temperature coefficient regime. Here, due to computational cost, a global scheme for n-heptane first proposed by Müller & Peters (1992) was selected and validated against ignition delay time data. The four-step mechanism approximates the overall behaviour of the low and high temperature chemical pathways.

IMPLEMENTATION

Numerical Method

The simulation was performed using the program S3D, see the publication by Chen *et al.* (2009) for full details. S3D solves the fully compressible Navier-Stokes, conservation of energy, conservation of mass, and conservation of species equations. Spatial gradients are evaluated using an eight-order central differencing scheme and the time advancement employs a fourth-order, six-stage explicit Runge-Kutta method. A Lewis number based transport model was used, as per Smooke (1991).

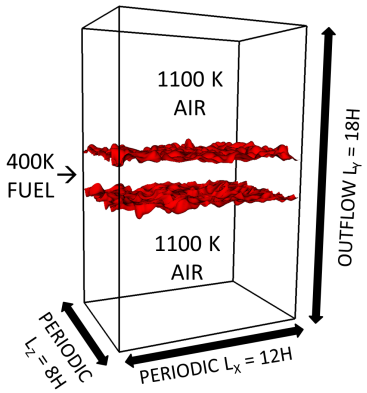

Figure 1. The domain extent and boundary conditions. The surface shows the stoichiometric mixture fraction surface at 10 jet times.

Configuration

The simulation consists of a plane-jet of fuel between stationary layers of oxidiser at a pressure of 40 atmospheres. The fuel is pure normal-heptane at 400 K and the oxidiser composition is 79% N_2 and 21% O_2 by volume at 1100 K. The jet has an initial width of H=0.233 mm and an initial centreline velocity of 7.49 ms^{-1}, which defines the jet time of t_{JET} = 31.1 μs. The profile of the jet in terms of the mixture fraction, Z, was: $Z(y) = 0.5\left(\tanh\left(\frac{y+H/2}{\sigma}\right) - \tanh\left(\frac{y-H/2}{\sigma}\right)\right)$, where the profile thickness, σ = H/8.

Superimposed on the initial condition was a spectrum of isotropic turbulence in order to trigger the Kelvin-Helmholtz instability of the jet. The isotropic turbulence had a velocity fluctuation scale of u'=0.375 ms^{-1} and an integral length scale of L_t = 77.7 μm.

The domain is summarised in Figure 1. The extent in the x, y, and z directions was L_x=12H, L_y=18H L_z=8H, respectively. The boundary conditions are periodic in the stream wise (x) and span wise (z) directions and non-reflecting outflow in the cross stream (y) direction, evaluated using the Navier Stokes characteristic boundary condition method (NSCBC), as developed by Poinsot & Lele (1992). The grid count in each direction is n_x=1440 , n_y=1472 , and n_z=960 which was selected to correctly resolve the smallest chemical and turbulent length scales. The resolution was deemed sufficient as judged by one- and two-dimensional grid convergence tests of flames under similar thermochemical conditions.

Tracer particles were embedded in the flow at the start of the simulation. Approximately 50 million particles were randomly inserted at a uniform density within the central half of the cross stream direction. The particles were convected with the flow but provided no feedback to the flow itself.

The duration of the DNS was 37 t_{JET}. The choice of H and U implies a jet Reynolds number of Re=9,000. The minimum ignition delay time, as calculated in zero-dimensional simulations, was τ_0=0.28 ms which defines a jet Damköhler number of Da=t_{JET}/τ_0=0.11. These values were selected in order to obtain an appropriately timed ignition in relation to the development of the jet.

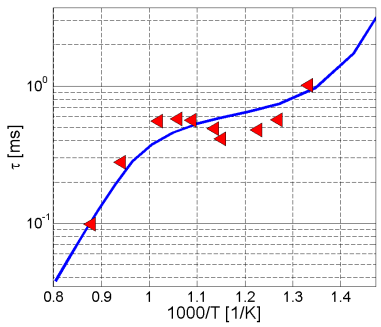

Figure 2. Validation of ignition delay times. Data points are experimentally values from Ciezki & Adomeit (1993), the blue line is obtained from the program SENKIN, developed by Lutz *et al.* (2002), using the rates detailed in table 1.

Chemistry

The chemical mechanism used is a 4-step global scheme, given by reactions R1 to R4, and is based on that published by Müller & Peters (1992). Species F represents the fuel, which is pure n-heptane. I, X, and P are lumped species. Species I is the low temperature intermediate, species X is the high temperature intermediate, and species P is the product mixture of CO_2 and H_2O.

Reactions R1 and R2 represent the high temperature chemical pathway. Reactions R3f and R4 represent the low temperature chemical pathway. The temperature dependence of reaction R3 controls the transition from low to high temperature pathways. The forwards R3f rate is favoured at low temperature and the backwards R3b rate is favoured at high temperatures. The temperature sensitivity is selected in order to approximate the observed negative temperature coefficient (NTC) region.

$$F \rightarrow X \quad \text{(R1)}$$
$$X + 11O_2 \rightarrow P \quad \text{(R2)}$$
$$F + 2O_2 \leftrightarrow I \quad \text{(R3)}$$
$$I + 9O_2 \rightarrow P \quad \text{(R4)}$$

The Arrhenius rates, presented in Table 1, were hand-tuned in order to obtain an improved agreement with experimental ignition delay time data from Ciezki & Adomeit (1993), see Figure 2.

The mechanism has short-comings compared to a detailed scheme, including:

1. It does not reproduce the NTC regime, it approximates it with a flattened, monotonic curve.
2. The action of radical species attacking the fuel and stable intermediate species, and its response to turbulence, are approximated by a purely thermally-driven process.

This mechanism was selected in spite of its shortcomings because it was the best candidate for investigating ignition at engine-relevant conditions, given the prohibitive computational cost of doing so with a detailed mechanism. The elevated pressure requires resolution of very small turbulent and chemical features. Additionally, to observe ignition, a sufficient number of ignition delay times (which imply a domain extent for a given target Re_{JET}) must be simulated. The range of scales implied by these two constraints leads to a computational cost between one and two orders of magnitude greater when using a detailed chemical mechanism as compared to the present global reaction scheme. This is due the increased number of chemical species and equations and, more importantly, the smaller length and time scales of the flame reaction zone.

Table 1. Arrhenius rates of 4-step n-heptane chemical mechanism .

Reaction	A [mol-cm-s-K]	E_a [K]
R1	1.2×10^{10}	19710
R2	2.0×10^{12}	7317
R3f	3.0×10^{18}	21650
R3b	4.0×10^{22}	34500
R4	3.8×10^{10}	6100

Lagrangian analysis

The passive, Lagrangian particles embedded within the Eularian field provide a convenient method for identifing and tracking the evolution of features of interest. In particular the autoignition locations (kernels) can be analysed by forming an ensemble of tracer particles co-located with the kernels at their time of formation. In doing so, the infinitesimal volume from which autoignition develops is approximated by set of sample points within finite volume. This approximation is a product of the limited resolution of the Lagrangian particles.

The following procedure is used to extract the Lagrangian information for the kernels:

1. A threshold heat release rate of HRR_T = -8.0×10^{11} Jm^{-3}s^{-1} is defined to identify the boundary between burning and non-burning regions in the domain.
2. By visually inspecting the surfaces of HRR_t over time, new kernels may be identified as newly-formed, closed surface elements which are distinct from any pre-existing burning surface. This task was performed using the visualisation software VisIt, developed by Childs *et al.* (2005).
3. The surface area and centroid of the kernel surface are calculated in order to define a particle search-volume.
4. For each kernel, particles are identified which reside within the search volume and exceed a threshold temperature (T > 1300 K) at its time of formation.
5. To avoid selection of particles belonging to a separate burning element, but to retain the correct morphology of the kernel, the particles are sorted in ascending order of temperature-weighted displacement ($\Delta_{T,i}$) from the kernel centroid. The temperature-weighted displacement is calculated as $\Delta_{T,i} = \Delta_i \left(c \left(\frac{T_{MAX} - T_i}{T_{MAX} - T_{MIN}} - 1 \right) + 1 \right)$, where c is a blending parameter from 0.0 (no temperature weighting) to 1.0 (full temperature weighting) and Δ_i is the particle displacement from the centroid. A value of c=0.7 was deemed appropriate for this study.
6. Given the sorted list of particles, the desired ensemble

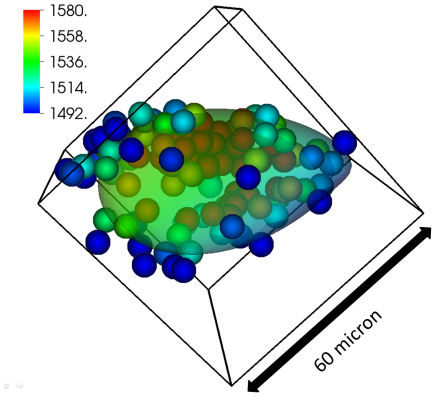

Figure 3. Example of particle ensemble for an ignition kernel. The surface is HRR_T coloured by temperature. The spheres are Lagrangian tracer particles coloured by temperature to the same colour scale.

size may be formed.

7. Ensemble members are identified based on a unique integer, they are used to sample the Eulerian field over time, thus providing the time-history statistics of the kernels.

An example ignition kernel, visualised by the HRR_T surface and its ensemble of particles, is shown in Figure 3.

RESULTS

Jet Development

The jet development, as described by the state of the Z_{ST} surface, is presented in Figure 4. The isotropic turbulence imposed at the initial condition rapidly triggers the Kelvin-Helmholtz instability of the jet. By about 10 jet times the shear driven turbulence is well-developed and mixing rates are near their peak value. As time progresses, the mixing rates relax and the integral length scales of the turbulence grow. By about 20 t_{JET}, the first autoignition event is observed. Multiple, discretely located autoignition events (kernels) form between 20 and 30 t_{JET}, by which time over half of the stoichiometric surface is burning. Based on initial observations, the ignition process is hypothosised as follows: the autoignition kernels expand as three-dimensional shells, they interact with the Z_{ST} surface and they establish edge-flames (partially premixed deflagrations), which propagate along the Z_{ST} surface. Between 30 and 37 t_{JET}, deflagration consumes most of the remaining unburnt Z_{ST} surface.

Conditional Averages

Statistics conditioned on Z were gathered. Figure 5 present maps of the conditional means of Temperature (T), scalar dissipation rate (χ), species I mass fraction (Y_I), and heat release rate (HRR) as they evolve in time.

The $\langle Y_I \mid Z \rangle$ profile shows that the low temperature chemistry (LTC) is initiated from a rich mixture fraction value of approximately Z=0.1. Between 0 and 10 t_{JET} the LTC moves into richer mixture fractions and $\langle Y_I \mid Z \rangle$ increases. By 10 t_{JET}, the shear turbulence has developed and resulted in mixing rates attaining their peak values. This is associated with an inhibition of the LTC as judged by a reduction in $\langle Y_I \mid Z \rangle$ magnitude and the slowed progress of

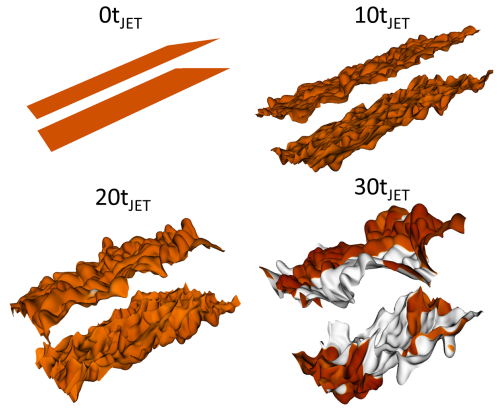

Figure 4. Evolution of Z_{ST} surface with time. Surface is coloured by temperature threshold. Orange colour indicates non-burning, white indicates burning (T > 1500 K).

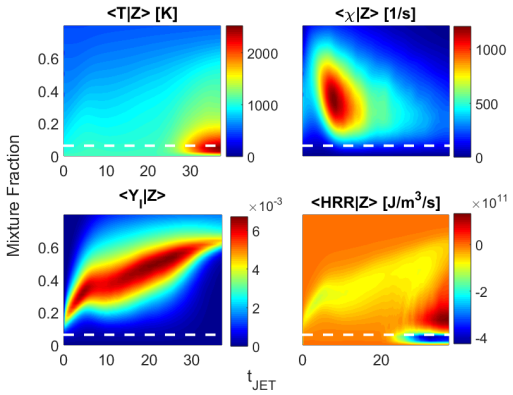

Figure 5. Maps of conditionally averaged quantities over time: top left, temperature (K); top right, scalar dissipation rate (s^{-1}); bottom left, species I mass fraction; bottom right, heat release rate ($Jm^{-3}s^{-1}$). The white dashed line marks the stoichiometric mixture fraction.

peak $\langle Y_I \mid Z \rangle$ into increasingly richer mixtures. As mixing rates relax, the LTC recovers and continues to move into richer mixtures. The $\langle$ HRR $\mid$ Z $\rangle$ and $\langle$ T $\mid$ Z $\rangle$ profiles show a transition to high temperature chemistry (HTC). By 30 t_{JET}, strong heat release and high temperature is observed about the Z_{ST} value. Based on preliminary observations, this is beleived to be associated with the development and propagation of edge-flames that were generated by the autoignition kernels (not shown here).

The conditionally-averaged statistics suggest that the overall ignition process is one in which a two-stage autoignition process leads to the formation of edge-flames and that both combustion modes are of significant importance. However, these results leave many questions unanswered, including:

1. What is controlling the autoignition timing?
2. Where in phase space the autoignition occurs?
3. What is the role of mixing?

The available Lagrangian particle data is leveraged with a view to address these questions.

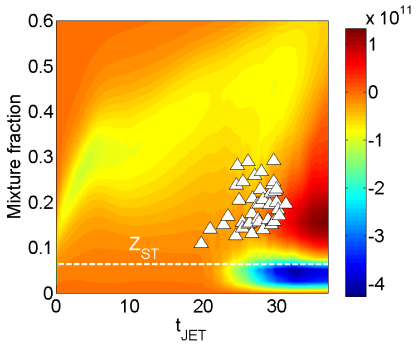

Figure 6. Lower right subplot from Figure 5, superimposed with the ignition timing and location in mixture fraction space for each kernel (white triangle markers).

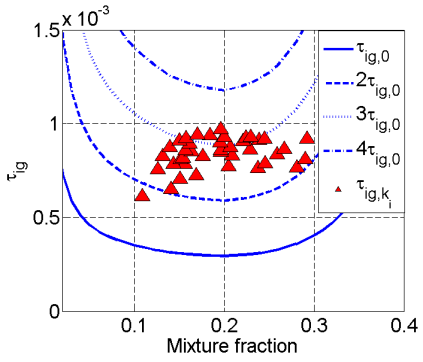

Figure 7. Red triangle markers show kernel ignition delay times. Blue lines show zero-dimensional ignition delay times multiples.

Kernel formation

Forty kernels are identified in this case. Their formation is mapped to t_{JET}-Z space in Figure 6, according to kernel-averaged values of Z, denoted $\langle Z \rangle_k$.

All kernels are formed between $\langle Z \rangle_k$=0.1 and $\langle Z \rangle_k$=0.3, and between 19 and 31 t_{JET}. The second stage of autoignition is occurring in very rich mixtures, but much less rich than the first stage of autoignition.

The temporal distribution of kernels is not uniform. The first five kernels are formed in about the same time as the last thirty five kernels, with the later kernels being much more broadly located in $\langle Z \rangle_k$ space.

A useful concept, introduced by Mastorakos *et al.* (1997), is that of the most reactive mixture fraction, Z_{MR}, which corresponds to the mixture fraction value at the point of minimum ignition delay time, τ_{MR}. Using this definition, the Z_{MR} = 0.11 and τ_{MR} = 19.7 t_{JET} in the present configuration. It is worth noting that due to the broad t_{JET}-Z distribution of kernels, the average kernel formation coordinates are a poor predictor of the τ_{MR} and Z_{MR}.

The kernel formation was also compared to zero-dimensional simulations conducted for a homogenous, constant pressure reactor using the program SENKIN, developed by Lutz *et al.* (2002). The comparison is presented in Figure 7. The $\langle \tau \rangle_k$ values reside between 1.8 and 3.4 times their respective τ_0 values, meaning that the action of spatial composition gradients and turbulence is to prolong the ignition delay time, and that the τ_0 values are not a very accurate predictor of the actual Z_{MR} and τ_{MR} values in this more realistic configuration.

Two kinds of kernels can be identified, based on their initial Z probability density functions (PDF). Kind 1 kernels are uniformly pure oxidiser at 0 t_{JET}, while kind 2 kernels have some degree of bimodality in their initial Z PDF. Figure 8 plots $\langle \tau \rangle_k$ against the initial kernel mean and kernel root-mean-square (RMS) Z values. A significant spread of ignition delay times are observed both kind 1 and 2 kernels. There is a negative correlation between initial Z mean and RMS, and $\langle \tau \rangle_k$. Kernels that initially contain fuel-rich modes in their PDF are more likely to ignite earlier, in particular kernel with the shortest $\langle \tau \rangle_k$ was also the richest and highly bimodal at the initial condition.

Kernel ignition trends

To understand the distribution of $\langle \tau \rangle_k$, tests for correlations were conducted based on the kernel statistics.

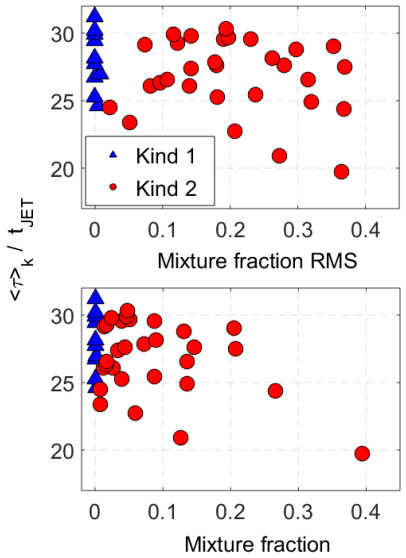

Figure 8. Ingition delay time against initial kernel mixture fraction RMS (top) and initial kernel mean mixture fraction (bottom). Blue triangle markers indicate kind 1 kernels, red circle markers indicate kind 2 kernels.

The strongest correlating factor for $\langle \tau \rangle_k$ was found to be the first stage ignition delay time, $\langle \tau_1 \rangle_k$, as shown in Figure 9. Earlier onset of the first stage of ignition leads to earlier second stage ignition with a nearly linear trend. This suggests that once the first stage is achieved, the second stage will proceed in a predictable manner (for those regions which lead to autoignition kernels). This seems reasonable given the rapid relaxation of mixing rates which follows the $\langle \tau_1 \rangle_k$ timing.

A correlation test conducted for the $\langle \tau_1 \rangle_k$ values found the most predictive factor was the timing of the peak in mixing rates, see Figure 9. In general, earlier peak mixing leads to earlier $\langle \tau_1 \rangle_k$. Two explanations are offered for this observation. Firstly, earlier mixing leads to earlier formation of appropriate Z values, and secondly, the sooner the mixing rates peak, the sooner they relax, allowing for the chemistry to proceed more quickly.

Other measurements of mixing, such as the peak value

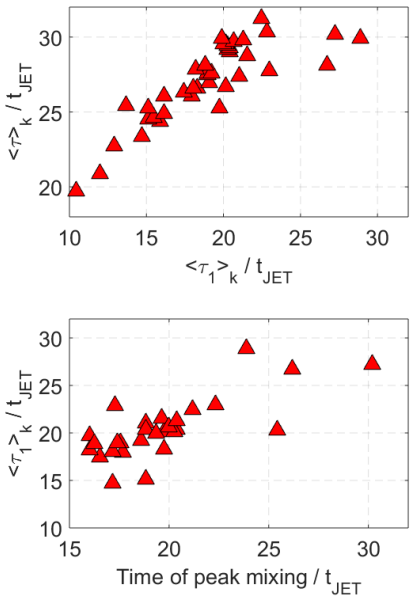

Figure 9. Upper figure: correlation between the timing of the second and first stages of autoignition, lower figure: correlation between the timing of the first stage of ignition and the timing of the peak in the kernel mixing rate.

of mixing rates or the cumulative mixing, were observed to be only weakly correlated with $\langle\tau\rangle_k$ or $\langle\tau_1\rangle_k$ (not shown).

CONCLUSIONS

A recent DNS study was conducted at diesel engine-relevant thermochemical conditions in the configuration of an igniting, temporally evolving jet using a four-step global n-heptane chemistry. An initially laminar but unstable jet is perturbed, leading to the development of shear-driven turbulence. Intense mixing rates inhibit the first stage of autoignition, before relaxing and then allowing the chemistry to proceed to the second stage of autoignition. Autoignition occurs within multiple discrete kernels that were widely distributed in space, time, and mixture fraction space. The kernels expanded, triggering edge-flame deflagrations where they intersected the stoichiometric mixture fraction surface and the combined effect of these burning modes tend towards a fully-burning state. Kernel-tracking analysis using Lagrangian tracer particles was conducted. The results suggest that the mixing history of the kernels controls the onset of autoignition and hence the overall ignition timing. In particular, earlier peaks in mixing are correlated with earlier onset of autoignition.

ACKNOWLEDGEMENTS

This work was supported by the Australian Research Council (ARC). The work at Sandia National Laboratories was supported by the Combustion Energy Frontier Research Center, an Energy Frontier Research Center funded by the US Department of Energy (DOE), Office of Science, Office of Basic Energy Sciences under Award No. DE-SC0001198. Sandia is a multiprogram laboratory operated by Sandia Corporation, a Lockheed Martin Company, for the United States Department of Energy under contract DE-AC04-94AL85000. This research used resources of the National Energy Research Scientific Computing Center, a DOE Office of Science User Facility supported by the Office of Science of the U.S. Department of Energy under Contract No. DE-AC02-05CH11231. The research benefited from computational resources provided through the National Computational Merit Allocation Scheme, supported by the Australian Government. The computational facilities supporting this project included the Australian NCI National Facility, the partner share of the NCI facility provided by Intersect Australia Pty Ltd., iVEC (Western Australia), and the UNSW Faculty of Engineering.

REFERENCES

Bhagatwala, A., Luo, Z., Shen, H., Sutton, J. A., Lu, T. & Chen, J. H. 2015 Numerical and experimental investigation of turbulent DME jet flames. *Proceedings of the Combustion Institute* **35** (2), 1157–1166.

Chen, J. H., Choudhary, A., de Supinski, B., DeVries, M., Hawkes, E. R., Klasky, S., Liao, W. K., Ma, K. L., Mellor-Crummey, J., Podhorszki, N., Sankaran, R., Shende, S. & Yoo, C. S. 2009 Terascale direct numerical simulations of turbulent combustion using S3D. *Computational Science and Discovery* **2** (1), 015001.

Childs, H., Brugger, E. S., Bonnell, K. S., Meredith, J. S., Miller, M., Whitlock, B. J. & Max, N. 2005 A contract-based system for large data visualization. In *Proceedings of IEEE Visualization 2005*, pp. 190–198.

Ciezki, H. K. & Adomeit, G. 1993 Shock-tube investigation of self-ignition of n-heptane-air mixtures under engine relevant conditions. *Combustion and Flame* **93** (4), 421–433.

Krisman, A., Hawkes, E. R., Bhagatwala, A., Talei, M. & Chen, J. H. 2014 A direct numerical simulation investigation of ignition at diesel relevant condition. In *Proceedings of 19th Australasian Fluid Mechanics Conference*. Melbourne, Australia.

Krisman, A., Hawkes, E. R., Talei, M., Bhagatwala, A. & Chen, J. H. 2015 Polybrachial structures in dimethyl ether edge-flames at negative temperature coefficient conditions. *Proceedings of the Combustion Institute* **35** (1), 999–1006.

Lutz, A. E., Kee, R. J. & Miller, J. A. 2002 Sandia national laboratories report no. sand87-8248.

Mastorakos, E., Baritaud, T. A. & Poinsot, T. J. 1997 Numerical Simulations of Autoignition in Turbulent Mixing Flows Lf. *Combustion and Flame* **109**, 198–223.

Müller, C. & Peters, N. 1992 Global kinetics for n-heptane ignition at high pressures. In *Twenty-Fourth Symposium (International) on Combustion/The Combustion Institute*, , vol. 20, pp. 777–784.

Pei, Y., Hawkes, E. R. & Kook, S. 2013 A Comprehensive Study of Effects of Mixing and Chemical Kinetic Models on Predictions of n-heptane Jet Ignitions with the PDF Method. *Flow, Turbulence and Combustion* **91** (2), 249–280.

Pickett, L.M. 2015 Engine combustion network data archive, <http://www.sandia.gov/ecn/index.php>.

Poinsot, T. J. & Lele, S. K. 1992 Boundary conditions for direct simulations of compressible viscous flows. *Journal of Computational Physics* **101** (1), 104–129.

Smooke, M. D., Giovangigli V. 1991 *Lecture Notes in Physics 384, Chap. 1*. New York: Springer-Verlag.